The influence of viral coding sequences on pestivirus IRES activity reveals further parallels with translation initiation in prokaryotes

The influence of viral coding sequences on pestivirus IRES activity reveals further parallels with translation initiation in prokaryotes

S. R. Fletcher, I. K. Ali, A. Kaminski, P. Digard and R. J. Jackson

RNA 2002 8: 1558-1571

RNA (2002), *8*:1558–1571. Cambridge University Press. Printed in the USA.

DOI: 10.1017/S1355838202023038

The influence of viral coding sequences on pestivirus IRES activity reveals further parallels with translation initiation in prokaryotes

SIMON P. FLETCHER,[1] IRAJ K. ALI,[1] ANN KAMINSKI,[1] PAUL DIGARD,[2] and RICHARD J. JACKSON[1]

[1]Department of Biochemistry, University of Cambridge, Cambridge CB2 1GA, United Kingdom
[2]Division of Virology, Department of Pathology, University of Cambridge, Cambridge CB2 1QP, United Kingdom

ABSTRACT

Classical swine fever virus (CSFV) is a member of the pestivirus family, which shares many features in common with hepatitis C virus (HCV). It is shown here that CSFV has an exceptionally efficient *cis*-acting internal ribosome entry segment (IRES), which, like that of HCV, is strongly influenced by the sequences immediately downstream of the initiation codon, and is optimal with viral coding sequences in this position. Constructs that retained 17 or more codons of viral coding sequence exhibited full IRES activity, but with only 12 codons, activity was ~66% of maximum in vitro (though close to maximum in transfected BHK cells), whereas with just 3 codons or fewer, the activity was only ~15% of maximum. The minimal coding region elements required for high activity were exchanged between HCV and CSFV. Although maximum activity was observed in each case with the homologous combination of coding region and 5′ UTR, the heterologous combinations were sufficiently active to rule out a highly specific functional interplay between the 5′ UTR and coding sequences. On the other hand, inversion of the coding sequences resulted in low IRES activity, particularly with the HCV coding sequences. RNA structure probing showed that the efficiency of internal initiation of these chimeric constructs correlated most closely with the degree of single-strandedness of the region around and immediately downstream of the initiation codon. The low activity IRESs could not be rescued by addition of supplementary eIF4A (the initiation factor with ATP-dependent RNA helicase activity). The extreme sensitivity to secondary structure around the initiation codon is likely to be due to the fact that the eIF4F complex (which has eIF4A as one of its subunits) is not required for and does not participate in initiation on these IRESs.

Keywords: classical swine fever virus (CSFV); eIF4A; hepatitis C virus (HCV); internal initiation of translation; IRES; RNA helicases

INTRODUCTION

Internal initiation of translation was first discovered in the animal picornavirus RNAs (Jang et al., 1988; Pelletier & Sonenberg, 1988), but has since been extended to hepatitis C virus (Tsukiyama-Kohara et al., 1992; Wang et al., 1993; Fukushi et al., 1994; Reynolds et al., 1995; Rijnbrand et al., 1995), and subsequently to the closely related pestiviruses (Poole et al., 1995; Rijnbrand et al., 1997; Pestova et al., 1998), as well as a few cellular mRNAs. It requires a substantial *cis*-acting RNA element generally known as the internal ribosome entry segment (IRES), about 450 nt long in the case of the picornaviruses and 300–330 nt in hepatitis C virus (HCV) and the pestiviruses. The mechanism of internal initiation is distinctly different for HCV and pestivirus IRESs as opposed to picornavirus RNAs. Small (40S) ribosomal subunits can bind directly to the HCV and pestivirus IRESs at the correct site even in the absence of any translation initiation factors (Pestova et al., 1998; Kieft et al., 2001), whereas the presence of factors is needed for small ribosomal subunit binding to picornavirus IRESs. Consequently, initiation on the HCV and pestivirus IRESs does not require eIF4A, 4B, 4E, or 4G, nor ATP hydrolysis (Pestova et al., 1998), in contrast to the picornavirus IRESs, which require eIF4A, 4B, and at least the central domain of eIF4G as well as ATP (Pestova et al., 1996a, 1996b). Thus, at the superficial operational level, initiation on the HCV IRES is similar to initiation of translation of prokaryotic mRNAs, but with a complex 330 nt IRES apparently playing a role analogous to the prokaryotic Shine–Dalgarno sequence.

Reprint requests to: Dr. Richard J. Jackson, Department of Biochemistry, University of Cambridge, Old Addenbrooke's Site, 80 Tennis Court Road, Cambridge CB2 1GA, United Kingdom; e-mail: rjj@mole.bio.cam.ac.uk.

The nature of the coding sequence downstream of the IRES generally has a rather modest influence on picornavirus IRES efficiency (Hunt et al., 1993), although more recently a fourfold effect on hepatitis A virus (HAV) IRES efficiency was seen if a length of HAV coding sequence greater than 66 nt was retained (Graff & Ehrenfeld, 1998). In contrast, it was found that retention of the 5′-proximal viral coding sequences was absolutely essential for HCV IRES activity (Reynolds et al., 1995). This result, which was obtained with two different reporters fused to the viral sequences, was considered very surprising at the time, but was subsequently reproduced with an entirely different reporter (Zhao et al., 1999). However, the claim for such a strong influence of coding sequences on IRES activity remained controversial, because what appeared to be high activity was observed with CAT or (firefly) luciferase reporters fused directly to the HCV initiation codon with no viral coding sequences retained (Tsukiyama-Kohara et al., 1992; Wang et al., 1993; Honda et al., 1996; Rijnbrand et al., 1997). Nevertheless, even with these two reporters, higher expression has subsequently been observed by some authors (Hahm et al., 1998; Hwang et al., 1998), though not others (Rijnbrand et al., 2001), if part of the 5′-proximal HCV coding sequences are retained and the reporter is fused to these rather than joined directly to the initiation codon.

In view of this controversy over the influence of viral coding sequences on HCV IRES activity, we decided to examine whether the retention of viral coding sequences influenced pestivirus IRES activity. Originally there were three recognized species of pestivirus, differing in their host animal: border disease virus (BDV), which infects sheep; bovine viral diarrhoea virus (BVDV); and classical swine fever virus (CSFV), formerly known as hog cholera virus. Subsequently, it has been determined that there are two types of BVDV (BVDV-1 and -2), which are classified as different species rather than different strains (Heinz et al., 2000). In addition, it has recently been shown that the pestiviruses isolated from reindeer and giraffes are each novel and distinct species (Avalos-Ramirez et al., 2001).

The experiments described here began with a study of the influence of various lengths of CSFV coding sequences on CSFV IRES activity. We then went on to test the effect of exchanging the HCV and CSFV coding sequences and linking them, in either orientation, to the heterologous 5′ UTR. The activity of these different hybrid IRES reconstructions was found to correlate with the absence of secondary structure in the immediate vicinity of the initiation codon. This finding echoes the independent observation that deliberate insertion of hairpin structures immediately downstream of the initiation codon is deleterious (Rijnbrand et al., 2001). However, the inhibitory structures in our constructs appeared to involve rather fewer base pairs than were in these inserted hairpins. We present evidence that this exquisite sensitivity to secondary structure in the vicinity of the initiation codon (which closely reflects the situation in prokaryotic systems) is a direct and probably inevitable consequence of the fact that initiation factors eIF4A and 4F do not participate in initiation on these IRESs.

RESULTS

The influence of viral coding sequences on CSFV IRES activity

To examine the influence of viral coding sequences on CSFV IRES activity, we effectively set out to map the 3′ boundary of the IRES, using the same approach as previously applied to the HCV IRES (Reynolds et al., 1995), and a very similar dicistronic test construct (pXLJ′0*S*), which has *Xenopus laevis* cyclin B2 cDNA as the upstream cistron and a downstream cistron coding for a slightly truncated form of the influenza virus NS1 protein (Borman & Jackson, 1992; Fletcher & Jackson, 2002). CSFV sequences to be tested for IRES activity were inserted between the *Sal*I and *Sna*BI sites in the short intercistronic cloning cassette of pXLJ′0*S* (Fig. 1; Fletcher & Jackson, 2002). As a preliminary, we compared the first 755 nt of the CSFV genome, generated as a *Sal*I-*Hin*dIII fragment as described in Fletcher and Jackson (2002), and the first 442 nt, a *Sal*I- (in-filled) *Age*I fragment (Fig. 1), each inserted so that the downstream NS′ reporter was in frame with the authentic CSFV initiation codon at nt 373 of the CSFV genomic sequence. In translation assays, the yield of IRES-dependent downstream cistron product was very similar in the two cases (data not shown), and thus if CSFV coding sequences contribute to the activity of the IRES, such sequences must lie entirely upstream of the *Age*I site, within the 5′-proximal 69 nt of viral coding sequences.

Accordingly, a series of 3′ deletions into the CSFV coding sequences from the *Age*I site was made, and the deleted fragments inserted between the *Sal*I and *Sna*BI sites of pXLJ′0*S* (Fig. 1). Capped and uncapped transcripts of these deletion constructs were then translated in the rabbit reticulocyte lysate system using a range of RNA concentrations. The results (Fig. 2) showed that although capping strongly influenced the yield of the cyclin product translated from the upstream cistron, it had no significant influence on the yield of IRES-dependent cistron product (NS′). Note that as there are approximately twice as many methionine residues in cyclin as in NS′, the molar yield of IRES-dependent cistron product is much higher than that of upstream scanning-dependent cistron product, even when the transcripts were capped. Thus the CSFV IRES was particularly efficient in this system, between fivefold and sixfold more efficient than the HCV IRES at RNA concentrations up to 50 μg/mL (see Fig. 5). As mentioned below, the CSFV IRES was also highly ef-

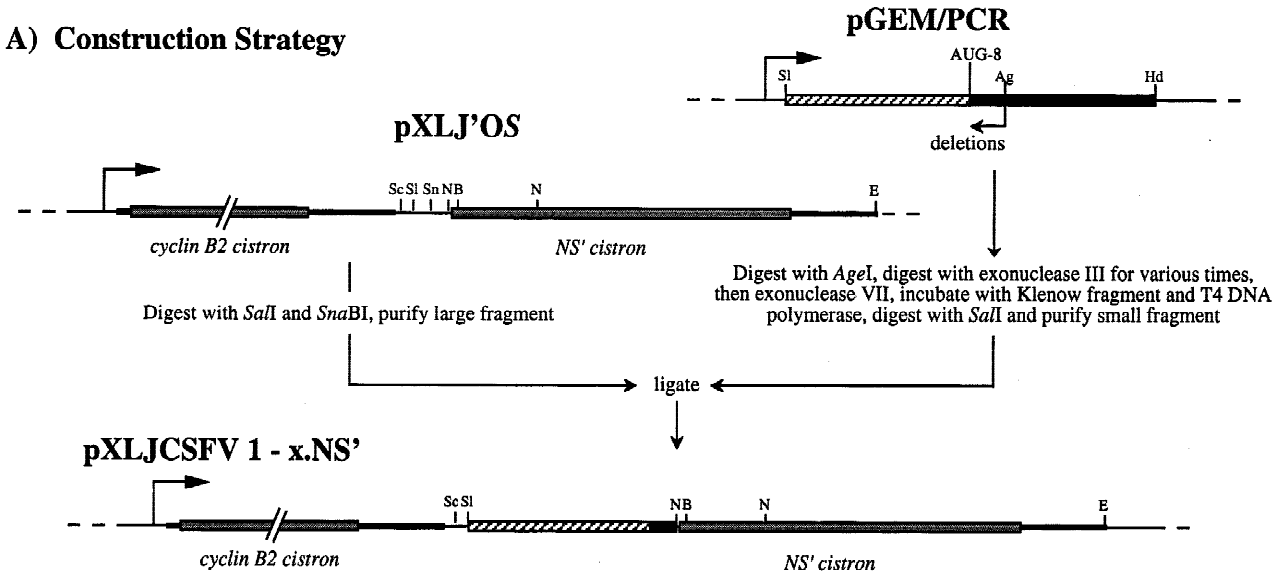

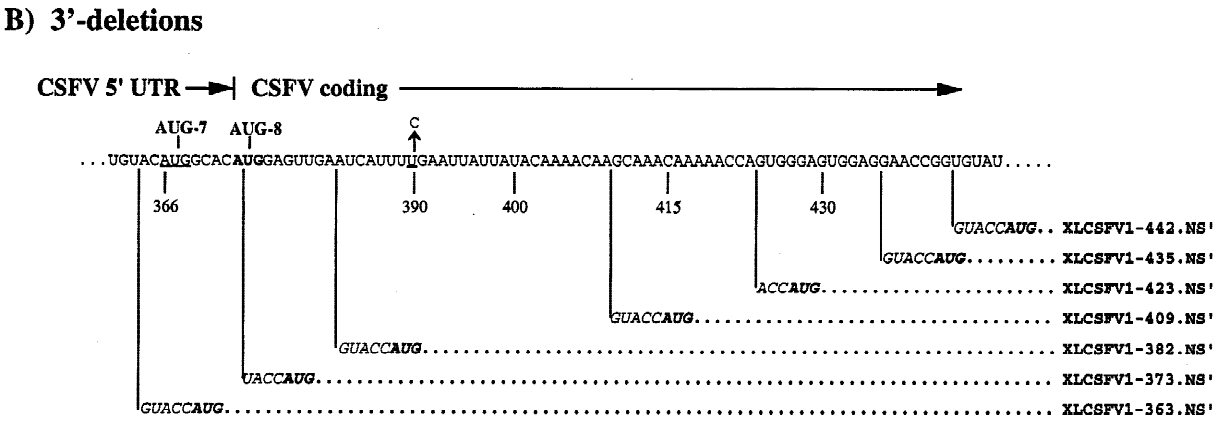

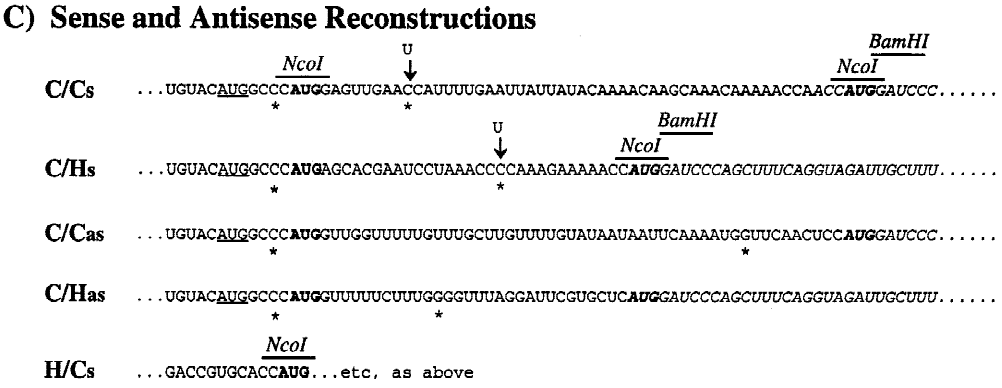

FIGURE 1. Construction strategy and sequence of critical constructs. **A:** Schematic diagram of the basic construction scheme. pGEM/PCR represents a cDNA copy of the first 755 nt of the CSFV genome cloned between the *Sal*I and *Hin*dIII sites of pGEM-1. pXLJ′0*S* has been described previously (Fletcher & Jackson, 2002). Thin lines denote vector or polylinker sequences, and thickened lines cyclin and NS′ 5′- or 3′-UTR sequences; the coding sequences of these two reporter cistrons are denoted by stippled rectangles, CSFV 5′-UTR sequences by a cross-hatched rectangle, and CSFV coding sequences by a filled (black) rectangle. Restriction enzyme sites are denoted as follows: Sc: *Sca*I, Sl: *Sal*I, Sn: *Sna*B1, N: *Nco*I, B: *Bam*HI, Ag: *Age*I, Hd: *Hin*dIII, and E: *Eco*RI. **B:** Sequences of the 3′-deletion constructs described herein. The numbering scheme corresponds to that of the CSFV genomic sequence. The authentic CSFV initiation codon (AUG-8) is shown in bold, and the upstream AUG-7 is underlined. Sequences of the NS′ reporter and its short upstream linker are italicized, with the AUG codon at the start of the NS1 ORF proper in bold italics. Unplanned deletions at the cut *Sna*B1 site occurred in the construction of pXLCSFV 1–373.NS′ and pXLCSFV 1–423.NS′ constructs. **C:** Sequences of the sense and antisense reconstructions derived from pXLCSFV 1–423.NS′. The ^{371}A → C mutation introduced to generate an *Nco*I site is shown by an asterisk just upstream of AUG-8. The other asterisks show, in the sense reconstructions, the U → C mutations introduced to avoid in-frame termination codons in the antisense orientation, where the corresponding positions are likewise indicated by an asterisk. The H/Cs reconstruction has exactly the same sequence downstream of the initiation codon (in bold) as C/Cs, and H/Hs the same as C/Hs.

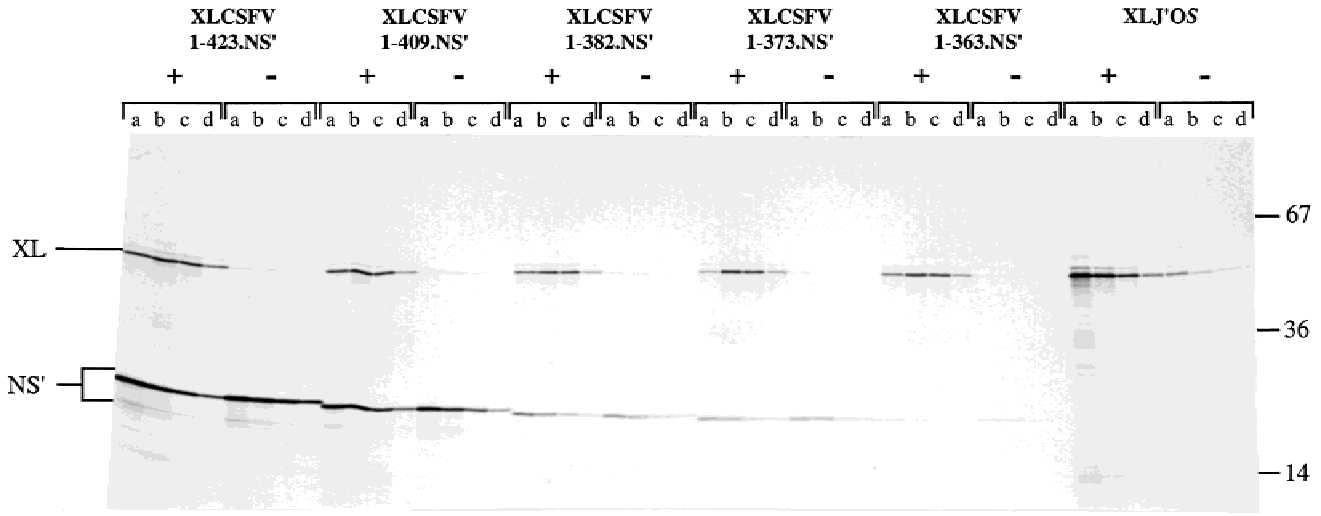

FIGURE 2. Mapping the 3′ boundary of the CSFV IRES by in vitro translation of capped and uncapped 3′-deletion mutants. Capped (+) and uncapped (−) transcripts of the designated constructs, which had all been linearized with *Eco*RI, were translated at concentrations of (a) 50, (b) 25, (c) 12.5, and (d) 6.25 μg/mL. The translation products were resolved on a 20% acrylamide gel, and the resulting autoradiograph is shown. XL indicates the cyclin B2 cistron translation product, and NS′ the product derived from the downstream cistron. The positions of the molecular weight markers (sizes in kilodaltons) are shown on the right.

ficient in transfected cells, but in this case only about two- or threefold better than the HCV IRES.

Inspection of Figure 2 shows that with progressively larger deletions from the 3′ end of the CSFV sequence there was a slight decrease in IRES activity as the deletion endpoint passed nt 423, followed by a sharper decrease as it passed nt 409. Because the authentic CSFV initiation codon is at nt 373–375, it is clear that viral coding sequences are important for the activity of the IRES, much as we found in the case of the HCV IRES (Reynolds et al., 1995). Particularly significant are the results of the pXLCSFV 1–373.NS′ mutant, which retains all of the CSFV 5′ UTR and the A of the initiation codon, but has no viral coding sequences whatsoever. The efficiency of internal initiation in this case was very low indeed, but it was not zero, in contrast to what was observed with almost the equivalent deletion in the case of HCV (Reynolds et al., 1995).

Figure 3 shows quantitative phosphorimaging data from an experiment similar to that in Figure 2, but using only uncapped RNA and including a construct with a greater length of coding sequence, pXLJCSFV 1–442.NS′. Constructs which retain just three codons of viral coding sequence (XLJCSFV 1–382.NS′), or have no coding sequence but the complete 5′ UTR (XLJCSFV 1–373.NS′), had only 10–15% of the maximum IRES activity, yet they were both definitely more active than XLCSFV 1–363.NS′, in which the deletion removes all coding sequences plus the last 9 nt of the 5′ UTR. XLCSFV 1–409.NS′, which retains 12 codons of viral coding sequence, exhibited about 66% of the max-

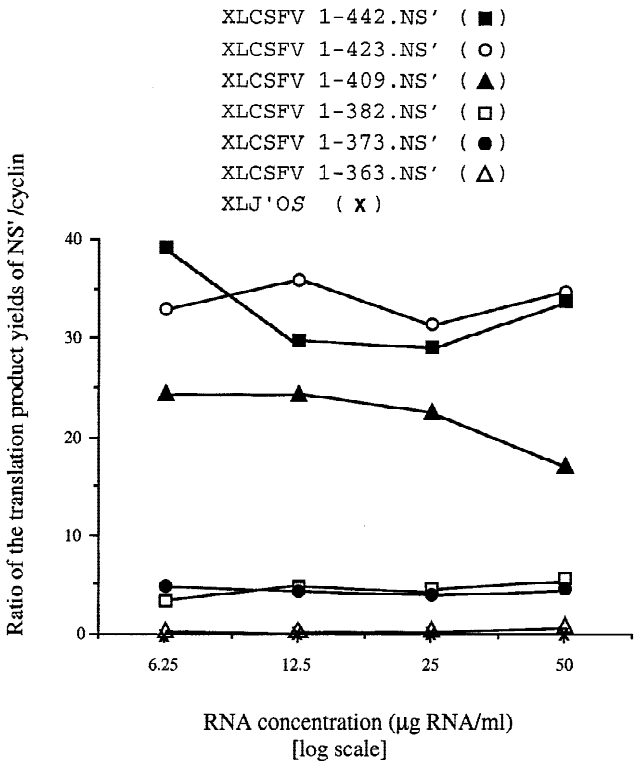

FIGURE 3. Quantitation of the in vitro translation assays of the 3′-deletion mutants. Uncapped transcripts of the designated constructs were translated at four different RNA concentrations as in Figure 2. Yields of radiolabeled cyclin and NS′ were determined by phosphorimaging; background intensity was defined for each individual band, and the integration was by volume. The ratio of the yield of NS′ to that of cyclin B2 for each mutant is plotted against RNA concentration, which is on a logarithmic scale.

imum IRES activity, whereas the 17 codons of XLCSFV 1–423.NS′ were sufficient to achieve this maximum. Thus the length of viral coding sequence required for full IRES activity in vitro is between 12 and 17 codons, whereas 10 codons were sufficient for maximum activity of the HCV IRES (Reynolds et al., 1995).

The same constructs were tested in transfected BHK-21 cells using infection with a recombinant vaccinia virus (vTF7-3) that expresses T7 RNA polymerase in order to drive transcription, as described previously (Reynolds et al., 1995). These assays produced further evidence for the extreme potency of the CSFV IRES in that in some experiments the NS′ protein product of translation of the IRES-dependent cistron could be seen as a major Coomassie-stainable band on gel electrophoresis of the cell extracts, despite the fact that the cyclin product from the upstream cistron was in such low abundance in these same experiments (presumably because of low transfection efficiency) that it could not be unambiguously detected as a radiolabeled protein following metabolic labeling using [^{35}S]methionine, and instead had to be detected and assayed by western blotting using an antibody specific for *Xenopus laevis* cyclin B2 and not cross-reactive with hamster cyclins. Figure 4 shows the results of a representative experiment. The relative IRES activities of the various deletion mutants determined as the ratio of radiolabeled NS′ signal to the cyclin signal on the Western blot were broadly similar to those obtained in the cell-free translation assays, differing only in minor details. XLCSFV 1–409.NS′ (12 codons of viral coding sequence) retained almost full IRES activity in vivo (as against 66% in vitro), whereas XLCSFV 1-382.NS′ (three codons) showed about 25% of maximum activity in vivo as compared with 15% in vitro. The two assays are thus in broad agreement, but it would seem that full IRES activity in vitro may require a slightly greater length of coding sequences than in vivo, and that deletion of almost all viral coding sequences may have a slightly more deleterious influence in vitro than in transfected cells. There is, however, the alternative possibility that because this transfection system generates such enormous quantities of RNA, subtle differences between the activity of different mutant IRES may be blurred. In addition, perhaps the activity of the full-length IRES may be underestimated simply because it is so very efficient that the system could be oversaturated.

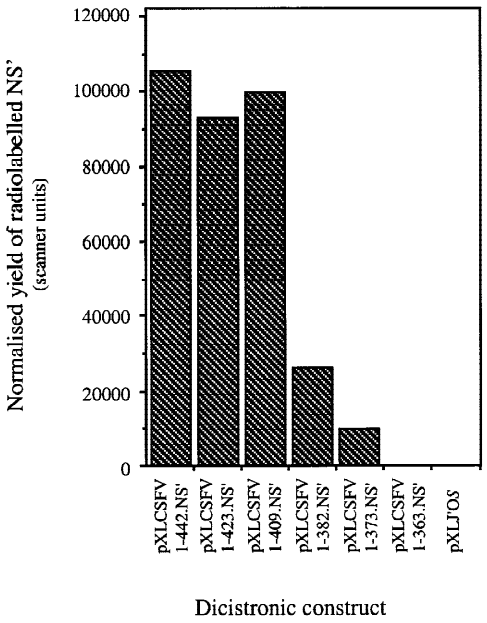

FIGURE 4. Mapping the 3′ boundary of the CSFV IRES by in vivo transfection assays. BHK-21 cells were infected with recombinant vaccinia virus (vTF7-3), which expresses bacteriophage T7 RNA polymerase, and were then transiently transfected with 5 μg of the designated plasmid DNAs. IRES activity was calculated as the ratio between expression of the downstream (IRES-dependent) cistron product (NS′) to the upstream cyclin B2 product, determined as described in Materials and Methods. Results from a representative experiment are shown.

The effect of interchanging CSFV and HCV coding sequences in both orientations

The sequences immediately downstream of the initiation codon of HCV and CSFV genomes code for different proteins: the core protein in the case of HCV, and a self-excising protease (N^{pro}) in CSFV. Thus the nucleotide sequences of the 5′-proximal part of the coding region are not the same in CSFV as in HCV, even though they share the common feature of being A rich and somewhat G poor (Fig. 1). It was therefore thought important to consider the question of whether high IRES activity was dependent strictly on the homologous combination of coding region and 5′ UTR. To this end, we exchanged the CSFV and HCV coding regions, not only in sense orientation but also in antisense, because we had previously found that if the coding region segment required for efficient HCV IRES function was inverted, no internal initiation occurred, which implied that the coding region was acting not just as a spacer, but was required per se (Reynolds et al., 1995).

Reconstructions with the HCV 5′ UTR were generated as described previously (Reynolds et al., 1995), using XL 40–339.NS′, which has no viral coding sequences, but retains all of the HCV 5′ UTR from nt 40 up to and including the initiation codon, and fortuitously has an *Nco*I site at the initiation codon. For reconstructions with the CSFV 5′ UTR, the starting construct was pXLCSV 1–423.NS′, but it was necessary to make a change in this to facilitate the reconstruction (Fig. 1). An A at the −2 position (numbered in relationship to the A of the initiation codon as +1) was mutated to a C residue, to generate an *Nco*I site overlapping the initiation codon. In addition, the oligonucleotides inserted to generate the sense reconstruction carried a muta-

tion that would change the fourth codon from AAU to AAC, so as to avoid introducing an in-frame termination codon in the antisense orientation reconstruction (Fig. 1). These two changes were found to reduce the IRES activity of the sense reconstruction, with a CSFV 5′ UTR (carrying a single mutation in the −2 position) and the CSFV coding sequences with an altered fourth codon, by about 15% with respect to wild-type XLCSFV 1–423.NS′. Consequently, all other results were compared with the sense reconstruction, which will be referred to as C/Cs denoting a CSFV 5′ UTR fused to the CSFV coding sequence element with the latter in the sense orientation.

The efficiency of internal initiation of translation of the downstream cistron of these reconstructions was assessed by in vitro translation of capped transcripts over a range of RNA concentrations (Fig. 5). The yields of labeled cyclin and NS′ in each assay were determined by scanning densitometry of each lane, and the ratio of the two yields calculated as a measure of IRES efficiency. For each reconstruction, the relative IRES efficiency at each RNA concentration was determined (with the efficiency of C/Cs set at 100%), and the average relative efficiency over all four RNA concentrations was calculated. This was found to be about 75% in the case of C/Hs, 45% for C/Cas, and less than 15% for C/Has. Over the complete RNA concentration range, the differences tended to be greatest at low RNA concentrations and smallest at high levels.

We also examined the reciprocal case of substituting 51 nt of CSFV coding sequences for the 33 nt of HCV coding sequences in the background of an IRES in which the 5′-UTR element is from HCV (Fig. 5). Again, the dicistronic mRNAs were assayed over a range of RNA concentrations to determine the relative efficiency of downstream cistron translation at each RNA concentration, and the average of the four values for relative efficiency was calculated. This gave an average relative efficiency for the H/Cs reconstruction of just under 50% relative to the H/Hs reconstruction. Thus maximum activity in both cases was seen with the homologous combination of coding sequence and 5′ UTR. However, sufficient activity was seen with heterologous combinations that it cannot be said that there is a strong and specific requirement for the homologous combination.

On the other hand, our previous conclusion that the coding region function is more than just that of a spacer is reinforced by the fact that CSFV coding sequences in the antisense orientation are relatively inefficient, and HCV coding sequences in reverse orientation very inefficient, in supporting CSFV IRES activity.

Probing the structure of the reconstructed IRESs

Alignment of the required segments of HCV and CSFV coding sequences, including alignment with the antisense orientations of these sequences, reveals very few exact matches between the coding sequences of the most active reconstructions (Fig. 1). Rather, there seems to be a general correlation between activity and

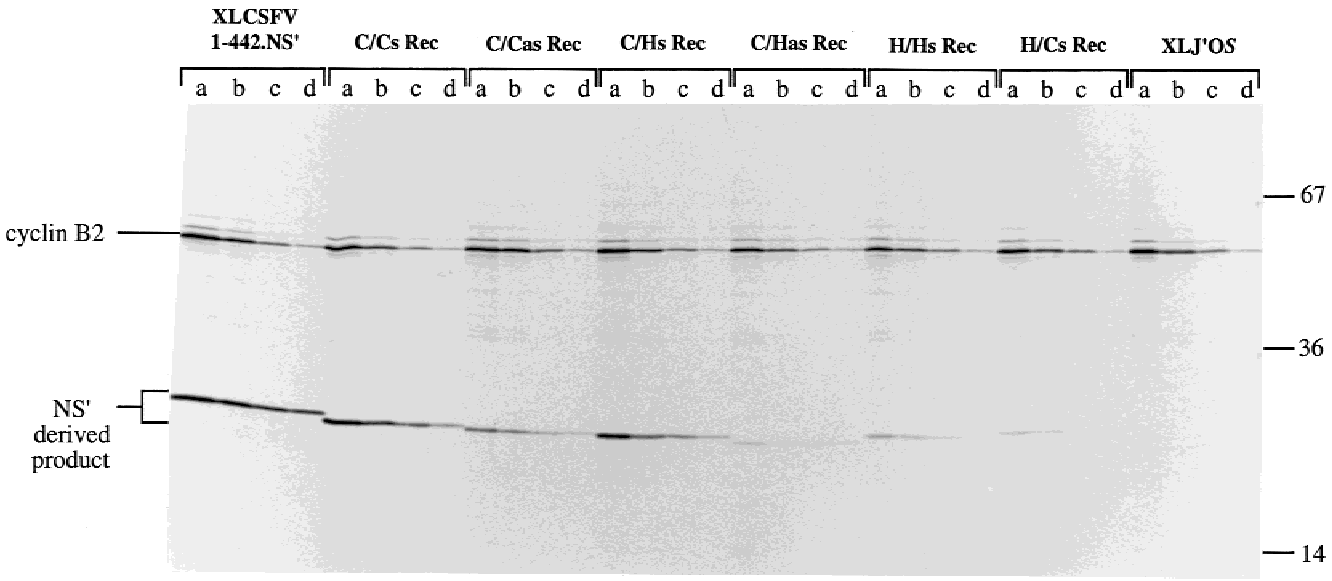

FIGURE 5. Hybrid CSFV and HCV IRESs with interchanged coding region segments still direct efficient internal initiation. Capped transcripts of constructs pXLCSFV 1–442.NS′, pXLJ′0*S* and the reconstructions C/Cs, C/Cas, C/Hs, C/Has, H/Hs, and H/Has (Fig. 1) were translated at final concentrations of (a) 50, (b) 25, (c) 12.5, and (d) 6.25 μg/mL. The translation products were resolved on a 20% acrylamide gel, and the resulting autoradiograph is shown. The upstream cyclin B2 cistron product is indicated, and NS′ indicates the product derived from the downstream cistron. The positions of the molecular weight markers (sizes in kilodaltons) are shown on the right.

the frequency of A residues. The number of A residues in the first 51 nt of coding sequences immediately following the AUG initiation codon (a length that includes part of the NS′ coding sequence in the case of the sense and antisense reconstructions with the HCV coding element) is: C/Cs 25, C/Hs 20, C/Cas 12, and C/Has 7. There is perhaps an even better correlation with clustering of A residues, which can be crudely indexed as the number of A residues that are followed by another A, and gives the following numbers for the first 51 nt: C/Cs 13, C/Hs 9, C/Cas 6, and C/Has 0. There is also a negative correlation between IRES efficiency and the frequency of G residues over this region.

However, these are only correlations between activity and the general primary sequence character of the coding region. There are few exact matches suggestive that a particular primary sequence motif in a particular position downstream of the AUG initiation codon is important. Therefore, it is possible that the explanation lies more in secondary structure features than primary sequence motifs. To explore this, we have carried out structure probing experiments to compare the sense and antisense reconstructions. The C/Cs, C/Cas, C/Hs, and C/Has dicistronic RNAs were probed with either cobra venom nuclease (CV) at two concentrations, a mixture of RNases A and T1, dimethyl sulphate, or kethoxal (Fig. 6).

Because mutagenesis has shown that the base pairing in the pseudoknot is important for IRES activity (Rijnbrand et al., 1997; Fletcher & Jackson, 2002), we first looked for differences in the probing pattern of this region. In all four cases, there was a strong stop at ^{361}U and a weaker one at ^{360}C, where the reverse transcriptase was impeded by the barrier of Stem II of the pseudoknot. Not surprisingly, there are sites of CV cleavage upstream of this, within the pseudoknot itself. However, there were also cuts by RNase A and T1 (single-strand specific) in the 5′ side of Stem II of the pseudoknot, and at both extremities of the "lower" strand of Stem IA; moreover G residues in Stem II and at both ends of Stem IA were reactive towards kethoxal. This suggests that some "breathing" of the pseudoknot structure may occur, which would correlate with the fact that the CSFV pseudoknot is a much less formidable barrier to reverse transcriptase than is the HCV pseudoknot (Pestova et al., 1998). The pattern of all the bands in the probing reactions, whether due to reverse transcriptase stops, CV cuts, or single-strand-specific enzymes or reagents, were remarkably similar for all four constructs (Fig. 6), implying that there are no major differences in the structure of the pseudoknot. In addition, no major differences were seen upstream of the pseudoknot (data not shown).

Turning to the region downstream of the pseudoknot, in C/Cs (the most active of the four reconstructed IRESs), there was a moderate stop to reverse transcriptase just 5′ to the initiation codon, coupled with CV hits in the same region (Fig. 6A). Further downstream, a stronger stop to reverse transcriptase was found in codon 5, coupled with CV hits in codon 6. Thus the region from the start of the initiation codon through to the middle of codon 5 appears to be unstructured, and this is supported by the fact that all four G residues in this region were moderately reactive towards kethoxal, as were the Gs in codons 7 and 13 (Fig. 6B).

The C/Hs reconstruction gave fairly similar results. There were some CV hits in the first part of the initiation codon, and in codon 3, while further downstream in codon 8 there were reverse transcriptase stops and sites of cleavage by CV nuclease (Fig. 6C). Again all the G residues in codons 1, 2, and 3 were moderately susceptible to reaction with kethoxal, while the G residue in codon 9 was exceptionally reactive (Fig. 6D), which is consistent with the strong band resulting from cleavage by T1 RNase at this site (Fig. 6C).

The next reconstruction in the hierarchy of activity, C/Cas, was rather different. Not only was there a stronger reverse transcriptase stop than in C/Cs or C/Hs on the 5′ side of the initiation codon, but there were other reverse transcriptase stops and CV cleavages in codons 2, 3, and 4 (Fig. 6A). It also seemed that although the first G in codon 3, and possibly also the second one, were reactive towards kethoxal, the G in the initiation codon was not (Fig. 6B). Further downstream, the strong CV cuts in codons 8 and especially 9 are indicative of secondary structure in this region, and there were weaker CV cuts in codons 13 and 14 (Fig. 6A). Consistent with this interpretation, the Gs in codons 8 and 9 did not seem to react with kethoxal, whereas those in codons 5 and 6 did, but only weakly (Fig. 6B).

FIGURE 6. Structure probing of the region around the IRES initiation codon of (**A**, **B**) C/Cs and C/Cas, (**C**, **D**) C/Hs and C/Has dicistronic RNAs. Reverse transcription was primed from a short distance downstream of the start of the NS′ ORF of the designated RNAs which had previously been subjected either (**A**, **C**) to cleavage by either CV nuclease (0.05 or 0.2 U/20 μL reaction as indicated), or RNase T1 together with RNase A (AT1), or (**B**, **D**) to chemical modification by either dimethyl sulfate or kethoxal, as described in Materials and Methods. Dideoxy sequencing of the construct DNA with the same oligonucleotide is also shown; although the direct read-out of the sequencing gel gave the sequence of the complementary strand, the labeling of the tracks (A, G, C, and T) in the figure has been switched so that the read-out now gives the sequence of the sense transcript. The codons between the viral initiation codon (AUG-8) and the start of the NS′ ORF itself are numbered in both margins, counting AUG-8, the initiation codon, as codon 1. In addition, the left margin has reference points to the various motifs that make up the pseudoknot structure, as defined in Fletcher and Jackson (2002).

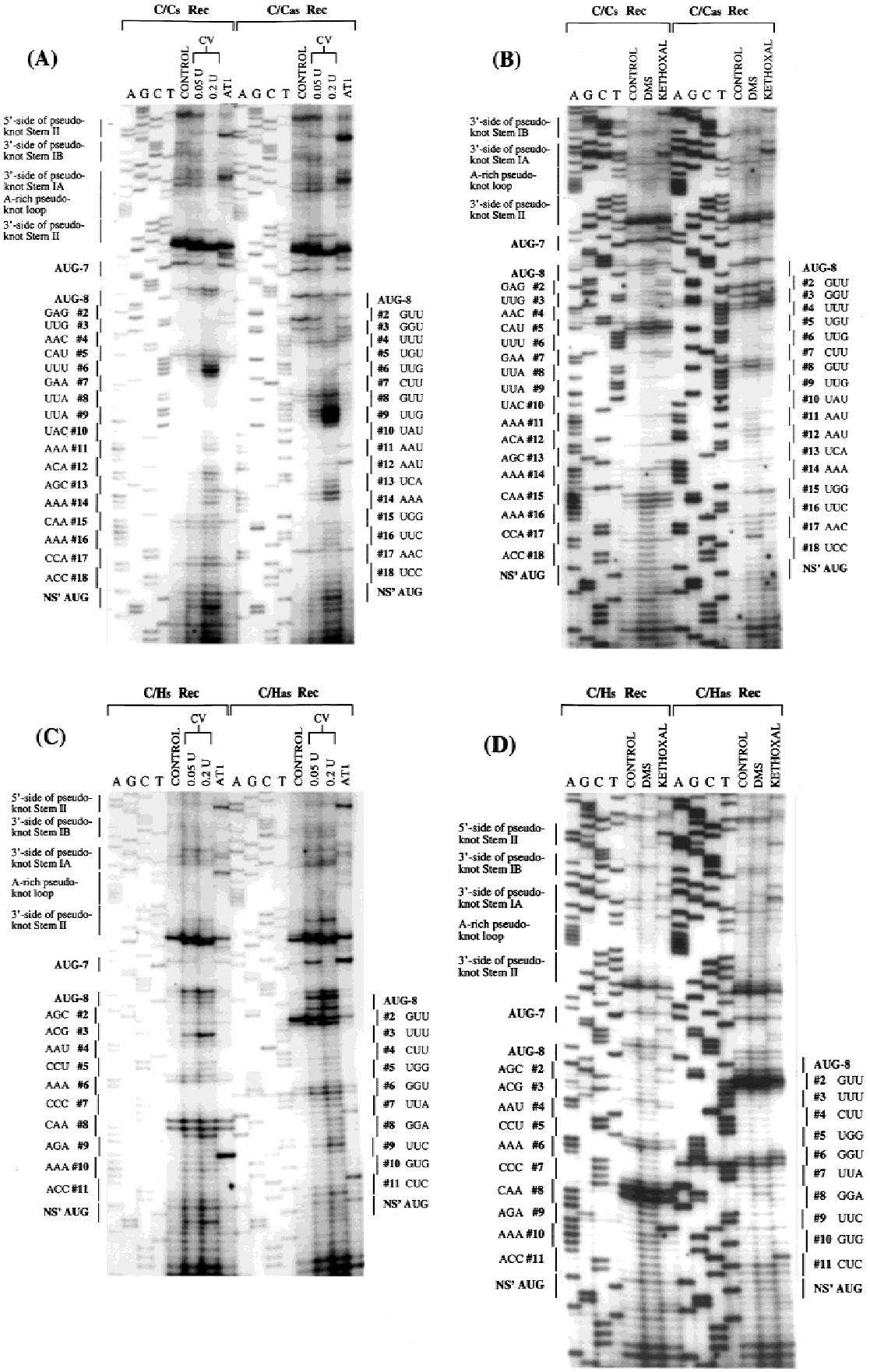

FIGURE 6. *See caption on facing page.*

Finally, the low activity C/Has reconstruction showed a very strong reverse transcriptase stop in codon 2, coupled with CV cuts throughout codons 1 and 2 (Fig. 6C). In addition the two Gs in this region appeared to be unreactive towards kethoxal, although the reverse transcriptase stops would have precluded detection of a low level of reaction (Fig. 6D). Codon 6 acted as a weak barrier to reverse transcriptase, and there were CV cuts in this region too (Fig. 6C). Of the four G residues in codons 5 and 6, only the wobble position of codon 5 and possibly the first position of codon 6 were attacked by kethoxal (Fig. 6D). On the other hand, the wobble position of codon 10 was very reactive to kethoxal (Fig. 6D), which correlates with the strong RNase T1 cleavage at this site (Fig. 6B).

Taking these four structures together, the activity of the reconstructed IRESs correlated best with an absence of apparent secondary structure (absence of reverse transcriptase stops or CV cuts, but reactivity of G residues towards kethoxal) from about the middle of the initiation codon through to codon 3, conceivably codon 4. This criterion would unambiguously predict a hierarchy of activity in the order C/Cs $>$ C/Hs $>$ C/Cas $\gg$ C/Has, precisely what was observed (Fig. 5). It is also possible that appropriately located downstream secondary structure (as revealed by reverse transcriptase stops and CV cuts) could play a positive role by causing ribosomes to pause at the initiation codon. Such structure was found at codon 3 (weakly) and more strongly at codon 8 in C/Hs, but at codons 5 and 6 in C/Cs, which might be thought to be a more appropriate position to induce such a pause.

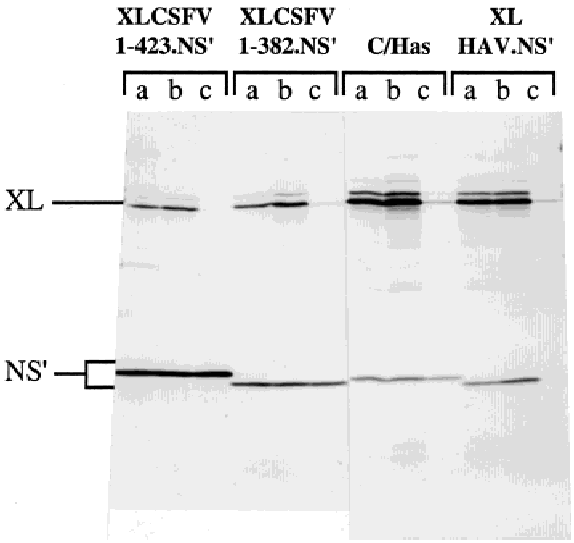

FIGURE 7. Supplementary eIF4A does not rescue the activity of defective mutant CSFV IRESs. Translation assays were carried out for 60 min with 25 μg/mL of the designated dicistronic mRNA without any supplementary eIF4A (a), in the presence of 250 μg/mL of supplementary recombinant wild-type eIF4A (b), or with 250 μg/mL R362Q dominant negative eIF4A (c; Pause et al., 1994). XLHAV.NS′ was included as a control: It is similar to the CSFV IRES constructs but has the hepatitis A virus (HAV) IRES, and is described by Borman et al. (1995). Translation products were separated by gel electrophoresis and detected by autoradiography. XL indicates the cyclin B2 cistron translation product, and NS′ the product derived from the downstream cistron.

The activity of defective IRESs cannot be rescued by increasing the concentration of eIF4A helicase

As the structure probing results suggest that even in the most inactive construct, C/Has, the secondary structure extends over only a few residues around the initiation codon, it is puzzling that what is apparently not very extensive secondary structure should be so strongly inhibitory. One possible explanation lies in the fact that initiation dependent on these IRESs does not require ATP hydrolysis, nor eIF4F, nor components of eIF4F such as eIF4A (an ATP-dependent RNA helicase) and eIF4E; nor do the HCV and CSFV IRESs seem to bind eIF4F or any of its constituent polypeptides (Pestova et al., 1998). As a consequence, translation dependent on these IRESs is unusual in its resistance to inhibition by dominant negative eIF4A mutants (Pestova et al., 1998), as confirmed in Figure 7. It is therefore doubtful whether there can be any focused unwinding of RNA around the initiation site through the action of the eIF4A helicase component of an eIF4F bound to a specific site in the IRES (Rozen et al., 1990).

If this is the case, then the only way that local secondary structure around the initiation codon could be unwound is by the action of singular eIF4A (though as this unwinding would probably not be directed or focused to the initiation site, it might not be very efficient). We therefore attempted to rescue the activity of two representative partially defective CSFV IRES mutants, XLJCSFV 1–382.NS′ and the C/Has reconstruction, by adding supplementary wild-type eIF4A to the translation assays, sufficient to raise the concentration to about threefold the level of endogenous eIF4A present in the lysate. However, this large excess of wild-type eIF4A failed to stimulate the mutant IRESs (Fig. 7). The eIF4A preparations were clearly active, as in some assays they slightly stimulated translation of the upstream cistron and translation dependent on the hepatitis A virus IRES control (Fig. 7), and they were shown to antagonize the inhibitory influence of the dominant negative eIF4A mutant on upstream cistron translation (data not shown). Because the helicase activity of eIF4A requires eIF4B in a type of cofactor role (Rozen et al., 1990), we also tested the effect of adding recombinant eIF4B together with the large excess of eIF4A, but again there was no stimulation or rescue of the mutant IRESs (data not shown).

DISCUSSION

We have shown here that, as with the HCV IRES (Reynolds et al., 1995), maximum activity of the CSFV IRES with NS′ as a reporter requires that some viral coding sequences are retained between the initiation codon and the reporter, even though the requirement is somewhat less stringent in the case of the more potent CSFV IRES. At first sight, the conclusion that viral coding sequences are required for maximum activity of both IRESs may be thought surprising, as others have obtained reasonably high activity when firefly luciferase or CAT reporters have been fused directly to the initiation codon, with no intervening viral coding sequences (Tsukiyama-Kohara et al., 1992; Wang et al., 1993; Honda et al., 1996; Rijnbrand et al., 1997). However, our results are not a peculiarity or artefact of the use of the influenza virus NS1 sequence as a reporter. There are no less than four other examples of different reporters that give zero or low (<25% of maximum) expression when fused directly to the initiation codon of either the HCV or CSFV IRESs (or both): *Renilla* luciferase (Laporte et al., 2000), secreted alkaline phosphatase (Reynolds et al., 1995), poliovirus VP4 coding sequences (Zhao et al., 1999), and HCV coding sequences in antisense orientation (Reynolds et al., 1995; Fig. 5). The five nonpermissive sequences have no obvious features in common.

On the other hand, apart from the actual viral coding sequences in sense orientation, there are just five different reporters that have been shown to give reasonably high activity when fused directly to the HCV or CSFV initiation codon (although two of these are not permissive for the closely related BVDV IRES): CAT, firefly luciferase, CSFV coding sequences in antisense orientation (Fig. 5), ubiquitin coding sequences in the case of the CSFV IRES (Tratschin et al., 1998), and CSFV internal sequences coding for NS3, as found in an autonomously replicating DI particle (Meyers & Thiel, 1995). However, attempts to construct or isolate analogous BVDV DI particles failed: Despite its close similarity to the CSFV IRES, the BVDV IRES evidently does not function if ubiquitin coding sequences or viral NS3 sequences are fused directly to the initiation codon. In the case of fusion to NS3, BVDV IRES activity could be rescued by mutations just downstream of the initiation codon (Myers et al., 2001). A viable replicon could also be constructed if some of the extreme 5′-proximal viral coding sequences were retained between the initiation codon and the ubiquitin cassette (Behrens et al., 1998). The length of N-terminal N^{pro} coding sequences required was greater than 12 nt but less than 84 (Behrens et al., 1998; Becher et al., 1999), and the structure of a natural helper-dependent DI suggests that 39 nt may be sufficient (Kupfermann et al., 1996).

Moreover, although CAT and firefly luciferase reporters have given good IRES activity when fused directly to the HCV or CSFV initiation codon (Tsukiyama-Kohara et al., 1992; Wang et al., 1993; Honda et al., 1996; Rijnbrand et al., 1997), this begs the question of whether their expression might not be higher if some viral coding sequences are retained between the initiation codon and the reporter ORF. In the case of a CAT reporter, retention of 30 nt or more of HCV coding sequences has been reported to stimulate expression between 2.5-fold and 4-fold in reticulocyte lysates, 10-fold in HeLa cell extracts, and between 2.5-fold and 6-fold in transfected HuH-7 cells (Hahm et al., 1998; Hwang et al., 1998). With a luciferase reporter in a monocistronic background, retention of 30 nt of HCV coding sequences stimulated expression about 6-fold both in vitro and in transfected HuH-7 cells (Hwang et al., 1998). On the other hand, more recently it has been reported that CAT expression was actually slightly higher in vitro and significantly greater in transfected cells if the reporter was fused directly to the HCV initiation codon than if 32 nt of viral coding sequences were retained (Rijnbrand et al., 2001). In the case of pestivirus IRESs, elimination of all viral coding sequences reduced the expression of a luciferase reporter from the BVDV IRES by just 20% in transfected cells (Chon et al., 1998), but the expression of CAT from the CSFV IRES in vitro was enhanced about 2-fold if 55 nt of viral coding sequences were retained (Rijnbrand et al., 2001). Although the effect of viral coding sequences is clearly complex, probably depending on the exact conditions used, it should be noted that there are more cases where retention of viral coding sequences caused a significant enhancement of CAT or luciferase expression than not. What is beyond question is that the activity of these IRESs can be profoundly influenced by the nature of the immediate downstream coding sequences, and as a general but not absolute rule, the authentic viral coding sequences support the highest activity.

It was therefore considered important to test whether the positive influence of coding sequences was restricted to IRESs with the homologous 5′ UTR, or whether the HCV and CSFV coding sequences were interchangeable. As a dedicated functional relationship restricted to the homologous combination of 5′ UTR and coding sequence would imply base pairing between the coding sequence and the UTR elements, we carried out structure probing in addition to functional assays with the heterologous combinations. Unfortunately the results of the functional assays were not completely unambiguous. The heterologous reconstructions were somewhat less active than the homologous, but were sufficiently active (provided the coding sequences were in sense orientation) that a highly specific or dedicated functional relationship between the coding sequence and the 5′ UTR seems very unlikely. This is consistent with the fact that the structure probing of the four permutations showed no significant differences upstream of the initiation codon (Fig. 6; data not shown).

What the structure probing did reveal was a strong correlation between IRES activity and absence of secondary structure interactions at the initiation codon and the following two or three codons (Fig. 6). In C/Has, and to a lesser extent C/Cas, this region is clearly involved in secondary structure interactions. Although we are unable to unambiguously deduce the actual base-paired structures, the absence of major differences in the probing patterns of all four RNAs in the region between the pseudoknot and the initiation codon (Fig. 6) suggests that the inhibitory structures are not akin to domain IV, discovered by Honda et al. (1996) in the wild-type HCV IRES, which is absent from (wild-type) pestivirus IRESs. The HCV domain IV involves base pairing between the extreme 3′ end of the 5′ UTR and the first part of the viral coding sequences, thus placing the AUG codon in the loop of a hairpin structure. On the basis of a mutagenesis study, it was suggested that the stability of domain IV has a negative correlation with HCV IRES activity (Honda et al., 1996), although others have argued that this alone cannot explain all the effects of mutations in the first part of the HCV ORF (Hwang et al., 1998).

A negative effect of secondary structure has also been invoked as the probable explanation for the inactivity of a BVDV replicon construct in which a large deletion fuses NS3 coding sequences to the initiation codon (Myers et al., 2001). Translation and autonomous RNA replication could be rescued by mutations in the early part of the NS3 sequence, and even a single G → U mutation 14 nt downstream of the A of the AUG was sufficient to convert an otherwise inactive construct into an active one. The effect of this mutation on the structure probing pattern was described as suggestive but inconclusive; the change specifically mentioned was more single-strandedness 16 residues from the A of the AUG (Myers et al., 2001), surprisingly right on the edge of the segment contacted by the initiating 40S subunit.

Given these effects of small changes in secondary structure, it is therefore not surprising that deliberate insertion of a quite substantial hairpin (−18 kcal/mol) immediately after the initiation codon and immediately upstream of a CAT reporter reduced IRES activity (Rijnbrand et al., 2001). Complete inhibition of the CSFV IRES was observed, but the reduction in HCV IRES activity was actually rather small (4-fold) in vitro, though greater than 10-fold in transfected cells. This HCV result is rather surprising given that mutations that marginally increase the stability of domain IV from its wild-type value of −6.2 kcal/mol to −8.1 kcal/mol also resulted in a ~4-fold decrease in translation (Honda et al., 1996). With both IRESs, inhibition by the hairpin insertion was decreased if 14 nt of viral coding sequences were retained between the AUG and the hairpin, and eliminated completely if 32 nt of viral coding sequence were retained (Rijnbrand et al., 2001).

The fact that a single mutation in the coding region can convert an inactive IRES–reporter construct into an active one (Myers et al., 2001) correlates with the fact that our structure probing data suggest that rather few residues around the initiation codon are involved in influencing the IRES activity, and thus the putative secondary structure in the inactive constructs cannot be very extensive. Why should what is probably rather modest secondary structure have such a serious influence on initiation dependent on the HCV or CSFV IRESs, when it has such a small influence on translation by the scanning ribosome mechanism of the same RNAs from which most of the viral 5′-UTR sequences have been deleted (Honda et al., 1996; Rijnbrand et al., 2001)? The answer almost certainly lies in the fact that initiation on these IRESs does not require ATP hydrolysis, nor eIF4A (an ATP-dependent RNA helicase), 4B, 4E, 4G, nor the eIF4F holoenzyme complex, consisting of eIF4A, 4E, and 4G (Pestova et al., 1998). It seems that these IRESs do not even bind eIF4F, which means that there is no possibility of its eIF4A subunit unwinding secondary structure in the vicinity of the binding site. In principle, unwinding might be effected by singular eIF4A and ATP, acting in conjunction with eIF4B. However, there are a number of problems with this suggestion: (1) the in vitro unwinding activity of singular eIF4A (plus ATP and eIF4B) is considerably less than that of eIF4F, eIF4B, and ATP (Rozen et al., 1990); (2) it is hard to see how singular eIF4A helicase activity could be directed to unwind specifically the region around the initiation site; and (3) the effects of dominant negative eIF4A mutants suggest that the role of eIF4A in initiation is mainly, if not exclusively, as a component of the eIF4F holoenzyme rather than as a singular entity (Pause et al., 1994). Consistent with these arguments, the direct test showed that a substantial increase in the concentration of singular eIF4A, with or without supplementary eIF4B, could not rescue the CSFV IRES constructs that had a low activity correlated with secondary structure around the initiation codon (Fig. 7).

In view of the mechanistic parallels between initiation in bacterial systems and initiation dependent on the HCV and CSFV IRESs (Pestova et al., 1998), it is interesting that this sensitivity to secondary structure is yet a further parallel. If the Shine–Dalgarno sequence and/or the initiation codon are involved in base-paired secondary structure weaker than −6 kcal/mol, there is no effect on initiation efficiency, but beyond this threshold there is a 10-fold decrease in initiation frequency for every additional −1.4 kcal/mol, exactly as predicted from theory (de Smit & van Duin, 1990, 1994b). The threshold value of about −6 kcal/mol is thought to reflect the 30S subunit/mRNA interaction and perhaps additionally mRNA/S1 ribosomal protein interaction displacing the equilibrium in favor of the unfolded state (de Smit & van Duin, 1994a), rather than the action of any of the numerous RNA helicases present in *Esche-*

richia coli (Kalman et al., 1991); and the close match with theoretical predictions implies that these helicases do not significantly unwind more stable structures at the initiation site, presumably because, like singular eIF4A, their action is rather disperse and is not specifically directed to that site. The consequence is hypersensitivity to secondary structure in the region contacted by the ribosome: The addition of just one extra base pair to a helix can reduce initiation frequency by at least 10-fold, even up to 1,000-fold, depending on the identity of the extra base pair and its immediate neighbors (de Smit & van Duin, 1994a, 1994b). Such extreme sensitivity to secondary structure has no known precedent in either the scanning ribosome mechanism or initiation dependent on picornavirus IRESs, but could explain the negative influence of rather limited secondary structure around the CSFV initiation codon reported here, and explain why a single mutation 14 nt downstream of the initiation codon can convert an inactive BVDV IRES into an active one (Myers et al., 2001).

The parallel with prokaryotic initiation is instructive, because a further feature of the prokaryotic system is that the nucleotide sequence or composition around the initiation site can also influence initiation efficiency. Contrary to popular opinion, a bacterial initiation site is more than just a Shine–Dalgarno motif located an appropriate distance upstream of an AUG or GUG codon. A statistical analysis has shown that the whole sequence between positions −20 and +15 with respect to the start site is nonrandom (Gold et al., 1981; Stormo et al., 1982). That there is additional information in this region has been confirmed by direct experimentation using an initiation site "trap" system, which was remarkable in its efficiency in selecting genuine initiation sites and rejecting sequences that fortuitously had a Shine–Dalgarno/AUG tandem (Dreyfus, 1988). Apart from the Shine–Dalgarno motif, no specific consensus sequence could be found for this region, but the general feature is that the genuine initiation sites are AT rich throughout, and especially A rich downstream of the initiation codon, features that could not be explained solely on the basis of evolutionary pressure counterselecting against internal self-complementarity. Interestingly, A-rich tracts are also found in the early part of the HCV and CSFV coding sequences, although for the most part they are more distant than 15 nt from the initiation codon.

Both the statistical analysis and the initiation site trap experiment show that the additional information in prokaryotic initiation sites only extends for about 15 nt downstream of the initiation codon. Thus, if coding sequences further downstream than +15 to +20 should affect the activity of the HCV and pestivirus IRESs, then the explanation most probably lies entirely in the influence of these sequences on RNA secondary structure around the initiation codon. If it is the first 15–20 nt downstream of the initiation codon that are influencing the efficiency of these IRESs, then although secondary structure could well be the explanation again, it might be premature to completely ignore the type of effects of nucleotide composition observed in the prokaryotic system. If there is this influence of nucleotide sequence/composition in prokaryotes, it would seem rather extraordinary that it would be completely absent in eukaryotes.

MATERIALS AND METHODS

Plasmid constructs

The CSFV fragment used to produce the constructs described in this study was originally obtained as construct pCSFV/5B generously donated by Drs. G. Meyers and H.-J. Thiel. This cDNA construct contained the first 1,248 nt of the CSFV Alfort Tübingen genome (accession number JO4358), including the first 9 nt at the 5′-terminal end of the sequence, which are missing from the original sequence of Meyers et al. (1989). PCR was used to amplify nt 1–826, with the forward primer designed to change the extreme 5′-terminal sequence from GTATAG to GTCGAC, in order to introduce a *Sal*I site. Following restriction digestion with *Sal*I and *Hin*dIII, the resulting product, which spanned nt 1–755 of the CSFV genome, was inserted into the corresponding sites of pGEM-1 (Promega), generating pGEM/PCR (Fig. 1). To generate deletions from the 3′ end of the CSFV sequence, pGEM/PCR was digested with *Age*I (between nt 438 and 439 of the CSFV sequence) and then with exonuclease III for various times, followed by exonuclease VII, as described by Henikoff (1987). The ends were in-filled using DNA polymerase I Klenow fragment, and then the CSFV sequence was released by digestion with *Sal*I and gel purified.

The control dicistronic construct, pXLJ′0*S*, used in this work is described in Fletcher and Jackson (2002). Downstream of a bacteriophage T7 promoter, it has a *X. laevis* cyclin B2 5′ UTR, coding region, and 3′ UTR, then a short cloning cassette with sites for *Sal*I, *Sac*I, *Sna*BI, and *Nco*I (in that order), followed by sequences coding for what is known as NS′, a slightly truncated form of the influenza virus (strain A/PR/34) NS1 protein described previously (Borman & Jackson, 1992), and finally the complete NS1 3′ UTR terminating in an *Eco*RI site (Fig. 1). The CSFV sequences were inserted between the *Sal*I/*Sna*BI sites of pXLJ′0*S*.

The point mutation $^{371}A \rightarrow C$ was made in pXLCSV 1–423.NS′, using the PCR method of Picard et al. (1994), incorporating modifications to the protocol as described by Kaminski and Jackson (1998). The mutation of nt 371 had the effect of generating a *Nco*I site at CSFV nt 371–376, which was used for interchanging of the CSFV and HCV coding sequences by a cloning strategy very similar to that of Reynolds et al. (1995).

All constructs were verified by dideoxynucleotide sequencing, and all plasmids were propagated by standard methods in *E. coli* TG1, using ampicillin selection (Sambrook et al., 1989).

In vitro transcription and translation assays

All plasmids were linearized by digestion with *Eco*RI prior to transcription (Fig. 1). The generation of capped or uncapped RNAs by transcription with bacteriophage T7 RNA polymerase, and the assay of these transcripts in the reticulocyte

lysate in vitro translation system with added KCl at 100 mM and Mg^{2+} at 0.5 mM, was exactly as described in Fletcher and Jackson (2002). Recombinant His-tagged wild-type and R362Q mutant eIF4A and wild-type eIF4B were expressed in *E. coli* BL21(DE3) and purified by Ni^{2+}-agarose affinity chromatography (Pause et al., 1994; Pestova et al., 1996a, 1998).

Transfection assays

Transfection assays were conducted as previously described (Fletcher & Jackson, 2002) using BHK-21 cells infected with recombinant vaccinia virus vTF7-3 (Fuerst et al., 1986). At 21 h posttransfection, metabolic labeling with [^{35}S]methionine (Amersham International) was carried out for 2 h, and the material then processed for gel electrophoresis. To detect and quantify the yield of cyclin, samples of cell extracts were subjected to western blotting using a mouse monoclonal antibody raised against *Xenopus* cyclin B2 (a gift of J. Gannon and T. Hunt), and alkaline phosphatase-conjugated goat anti-mouse secondary antibody, with quantitation of alkaline phosphatase activity as described in Fletcher and Jackson (2002).

Structure probing

RNA structural analysis was carried out using both single-strand- (A and T1) and double-strand- (CV) specific RNases, and also single-strand-specific chemical reagents (dimethyl sulfate specific for unpaired A and C residues, and kethoxal specific for unpaired G residues). For enzymatic probing, each 20-μL reaction was set up on ice and contained 4 μg uncapped RNA, either 10 U of freshly diluted RNase T1 (Boehringer) together with 0.005 μg of RNase A (Sigma), or either 0.05 or 0.2 U of freshly diluted RNase CV1 (Pharmacia) in 80 mM Tris-HCl, pH 7.8, 2.5 mM $MgCl_2$, 120 mM KCl. The reactions were incubated on ice for 30 min. The digestions were terminated by the addition of 3 vol of enzyme modification stop buffer: 0.3 M Na(OAc), 10 mM EDTA, pH 8.0, 10 μg calf liver tRNA (Boehringer); and 4 vol of phenol. After mixing and centrifugation, the upper aqueous layer was isolated, and the RNA extracted once with phenol and twice with chloroform and then precipitated with 3 vol of 96% ethanol. Following centrifugation, each pellet was taken up in RNA dilution buffer (7 mM $MgCl_2$, 25 mM DTT, 50 mM Tris-HCl, pH 8.0, 75 mM KCl), to give a final concentration of ~0.15 mg/mL.

For chemical modification, each 25-μL reaction contained 4 μg uncapped RNA and either 10.6 mM dimethyl sulfate or 0.5 μg/mL kethoxal in 120 mM KCl, 0.5 mM $MgCl_2$, 30 mM HEPES-KOH, pH 8.0. Reactions were incubated at 25 °C for 10 min, and then stopped by addition of 10 μg calf liver tRNA, 1 M NaOAc, 660 mM 2-mercaptoethanol, 660 mM Tris-HCl, pH 7.5, and an additional 25 mM potassium borate in the case of kethoxal modifications. Following ethanol precipitation, the RNA was purified by phenol extraction followed by chloroform extraction, reprecipitated, and taken up in the same buffer as for enzymatic modification. For the kethoxal modified RNA, 25 mM potassium borate, pH 7.0, was present in all buffers used in the workup.

Enzymatic cleavage and chemical modification sites were identified by primer extension with a 5′-end-labeled primer 5′-CTCGTTTGCGGACATGCC-3′ (complementary to the sense strand of a region of the NS′ ORF close to its 5′ end). Labeling of the primer was performed in a total volume of 10 μL, containing 10 pmol oligonucleotide, 10 U T4 polynucleotide kinase (New England Biolabs) and 5 μL [γ-^{32}P]ATP (Amersham International) in 50 mM Tris-HCl, pH 7.4, 10 mM $MgCl_2$, 5 mM DTT. The reaction was incubated at 37 °C for 30 min, stopped by heating to 65 °C for 5 min, and then stored on ice.

Annealing of the labeled primer with the RNA samples was performed in a total volume of 3 μL, containing 1 pmol end-labeled oligonucleotide and 0.2 μg RNA. The reaction was heated to 90 °C for 3 min and then placed immediately on ice to cool. After annealing, the reaction was preheated at 42 °C for 4 min and then the primer extended by the addition of 20 μM (final concentration) dNTPs, 21.3 mM DTT, and ~0.8 U AMV reverse transcriptase (Pharmacia). The reaction was incubated at 42 °C for 30 min, and reverse transcription was halted by the addition of an equivalent volume of room temperature stop dye (90% de-ionized formamide, 1 mg/mL bromophenol blue, 10 mM EDTA, pH 8.0). The cDNA samples were analyzed by 6% polyacrylamide/8 M urea gel electrophoresis and the fixed, dried gels were exposed to preflashed Fuji RX film. For markers, dideoxynucleotide sequencing reactions of the parent plasmid DNA from which the RNA had been transcribed were carried out using the same primer.

ACKNOWLEDGMENTS

We thank Drs. G. Meyers and H.-J. Thiel for the original gift of the CSFV 5′-UTR plasmid, and for advice; Tim Hunt and Julian Gannon for the gift of a highly specific antiserum raised against *X. laevis* cyclin B2; Nahum Sonenberg, Tatyana Pestova, and Christopher Hellen for the eIF4A expression constructs; Simon Morley for the eIF4B expression construct; Dr. Konrad Bishop for help with the transfection assays; and Catherine Gibbs for technical support. The costs of this work were supported mainly by a grant from the Wellcome Trust. S.P.F. and I.K.A gratefully acknowledge the support of research studentships awarded by the Medical Research Council.

Received April 16, 2002; returned for revision May 22, 2002; revised manuscript received September 9, 2002

REFERENCES

Avalos-Ramirez R, Orlich M, Thiel HJ, Becher P. 2001. Evidence for the presence of two novel pestivirus species. *Virology 286*:456–465.

Becher P, Orlich M, Konig M, Thiel HJ. 1999. Nonhomolgous RNA recombination in bovine viral diarrhea virus: Molecular characterization of a variety of subgenomic RNAs isolated during an outbreak of fatal mucosal disease. *J Virol 73*:5646–5653.

Behrens S-E, Grassmann CW, Thiel H-J, Meyers G, Tautz N. 1998. Characterization of an autonomous subgenomic pestivirus replicon. *J Virol 72*:2364–2372.

Borman A, Jackson RJ. 1992. Initiation of translation of human rhinovirus RNA: Mapping the internal ribosome entry site. *Virology 188*:685–696.

Borman AM, Bailly J-L, Girard M, Kean KM. 1995. Picornavirus internal entry segments: Comparison of translational efficiency and the requirements for optimal internal initiation *in vitro*. *Nucleic Acids Res 23*:3656–3663.

Chon SK, Perez DR, Donis RO. 1998. Genetic analysis of the internal ribosome entry segment of bovine viral diarrhoea virus. *Virology 251*:370–382.

de Smit MH, van Duin J. 1990. Secondary structure of the ribosome binding site determines translational efficiency—A quantitative analysis. *Proc Natl Acad Sci USA 87*:7668–7672.

de Smit MH, van Duin J. 1994a. Translational initiation on structured messengers: Another role for the Shine–Dalgarno interaction. *J Mol Biol 235*:173–184.

de Smit MH, van Duin J. 1994b. Control of translation by mRNA secondary structure in *Escherichia coli*: A quantitative analysis of literature data. *J Mol Biol 244*:144–150.

Dreyfus M. 1988. What constitutes the signal for initiation of protein synthesis on *Escherichia coli* mRNAs? *J Mol Biol 204*:79–94.

Fletcher SP, Jackson RJ. 2002. Pestivirus internal ribosome entry site (IRES) structure and function: Elements in the 5′ untranslated region important for IRES function. *J Virol 76*:5024–5033.

Fuerst TR, Niles EG, Studier FW, Moss B. 1986. Eukaryotic transient expression system based on recombinant vaccinia virus that synthesizes bacteriophage T7 RNA polymerase. *Proc Natl Acad Sci USA 83*:8122–8126.

Fukushi S, Katayma K, Kurihara C, Ishiyama N, Hoshin FB, Ando T, Oya A. 1994. Complete 5′ noncoding region is necessary for the efficient internal initiation of hepatitis C virus RNA. *Biochem Biophys Res Commun 199*:425–432.

Gold L, Pribnow D, Schneider T, Shinedling S, Swebilius-Singer B, Stormo G. 1981. Translation initiation in prokaryotes. *Annu Rev Microbiol 35*:365–403.

Graff J, Ehrenfeld E. 1998. Coding sequences enhance internal initiation of translation by hepatitis A virus RNA in vitro. *J Virol 72*: 3571–3577.

Hahm B, Kim YK, Kim JH, Kim TY, Jang SK. 1998. Heterogeneous nuclear ribonucleoprotein L interacts with the 3′ border of the internal ribosome entry site of hepatitis C virus. *J Virol 72*:8782–8788.

Heinz FX, Collett MS, Purcell RH, Gould EA, Howard CR, Houghton M, Moorman RJM, Rice CM, Thiel H-J. 2000. Family Flaviviridae. In: van Regenmortel MHV, Fauquet CM, Bishop DHL, Carstens EB, Estes MK, Lemon SM, Maniloff J, Mayo MA, McGeoch DJ, Pringle CR, Wickner RB, eds. *Virus taxonomy. Seventh Report of the International Committee on Taxonomy of Viruses*. San Diego, CA: Academic Press. pp 859–878.

Henikoff S. 1987. Unidirectional digestion with exonuclease III in DNA sequence analysis. *Methods Enzymol 155*:156–165.

Honda M, Brown EA, Lemon SM. 1996. Stability of a stem-loop involving the initiator AUG controls the efficiency of internal initiation of translation on hepatitis C virus RNA. *RNA 2*:955–968.

Hunt SL, Kaminski A, Jackson RJ. 1993. The influence of viral coding sequences on the efficiency of internal initiation of translation of cardiovirus RNAs. *Virology 197*:801–807.

Hwang LH, Hsieh CL, Yen A, Chung YL, Chen DS. 1998. Involvement of the 5′ proximal coding sequences of hepatitis C virus with internal initiation of viral translation. *Biochem Biophys Res Commun 252*:455–460.

Jang SK, Krausslich H-G, Nicklin MJH, Duke GM, Palmenberg AC, Wimmer E. 1988. A segment of the 5′ nontranslated region of encephalomyocarditis virus RNA directs internal entry of ribosomes during in vitro translation. *J Virol 62*:2636–2643.

Kalman M, Murphy H, Cashel M. 1991. RhlB, a new *Escherichia coli* K12 gene with an RNA helicase-like protein sequence motif, one of at least 5 such possible genes in a prokaryote. *New Biologist 3*:886–895.

Kaminski A, Jackson RJ. 1998. The polypyrimidine tract binding protein (PTB) requirement for internal initiation of translation of cardiovirus RNAs is conditional rather than absolute. *RNA 4*:626–638.

Kieft JS, Zhou K, Jubin R, Doudna JA. 2001. Mechanism of ribosome recruitment by hepatitis C IRES RNA. *RNA 7*:194–206.

Kupfermann H, Thiel H-J, Dubovi EJ, Meyers G. 1996. Bovine viral diarrhoea virus: Characterization of a cytopathogenic defective interfering particle with two internal deletions. *J Virol 70*:8175–8181.

Laporte J, Malet I, Andrieu T, Thibault V, Toulmé J-J, Wychowski C, Pawlotsky J-M, Huraux J-M, Agut H, Cahour A. 2000. Comparative analysis of translation efficiency of hepatitis C virus 5′ untranslated regions amongst intraindividual quasispecies present in chronic infection: Opposite behaviors depending on cell type. *J Virol 74*:10827–10833.

Meyers G, Rümenapf T, Thiel HJ. 1989. Molecular cloning and nucleotide sequence of the genome of hog cholera virus. *Virology 171*:555–567.

Meyers G, Thiel H-J. 1995. Cytopathogenecity of classical swine fever virus caused by defective interfering particles. *J Virol 69*:3683–3689.

Myers TM, Kolupaeva VG, Mendez E, Baginski SG, Frlov I, Hellen CUT, Rice CM. 2001. Efficient translation initiation is required for replication of bovine viral diarrhea virus subgenomic replicons. *J Virol 75*:4226–4238.

Pause A, Methot N, Svitkin Y, Merrick WC, Sonenberg N. 1994. Dominant negative mutants of mammalian translation initiation factor eIF-4A define a critical role for eIF-4F in cap-dependent and cap-independent initiation of translation. *EMBO J 13*:1205–1215.

Pelletier J, Sonenberg N. 1988. Internal initiation of translation of eukaryotic mRNA directed by a sequence derived from poliovirus RNA. *Nature 334*:320–325.

Pestova TV, Hellen CUT, Shatsky IN. 1996a. Canonical eukaryotic translation initiation factors determine initiation of translation by internal ribosome entry. *Mol Cell Biol 16*:6859–6869.

Pestova TV, Shatsky IN, Hellen CUT. 1996b. Functional dissection of eukaryotic initiation factor eIF4F: The 4A subunit and the central domain of the 4G subunit are sufficient to mediate internal entry of 43S preinitiation complexes. *Mol Cell Biol 16*:6870–6878.

Pestova TV, Shatsky IN, Fletcher SP, Jackson RJ, Hellen CUT. 1998. A prokaryotic-like mode of cytoplasmic eukaryotic ribosome binding to the initiation codon during internal translation initiation of hepatitis C and classical swine fever virus RNAs. *Genes & Dev 12*:67–83.

Picard V, Ersdalbadju E, Lu AQ, Bock SC. 1994. A rapid and efficient one-tube PCR-based mutagenesis technique using *Pfu* DNA polymerase. *Nucleic Acids Res 22*:2587–2591.

Poole TL, Wang C, Popp RA, Potgieter LND, Siddiqui A, Collett MS. 1995. Pestivirus translation initiation is by internal ribosome entry. *Virology 206*:750–754.

Reynolds JE, Kaminski A, Kettinen HJ, Grace K, Clarke BE, Carroll AR, Rowlands DJ, Jackson RJ. 1995. Unique features of internal initiation of hepatitis C virus RNA translation. *EMBO J 14*:6010–6020.

Rijnbrand R, Bredenbeek PJ, Haasnoot PC, Kieft JS, Spaan WJM, Lemon SM. 2001. The influence of downstream protein-coding sequences on internal ribosome entry on hepatitis C virus and other flavivirus RNAs. *RNA 7*:585–597.

Rijnbrand R, Bredenbeek P, van der Straten T, Whetter L, Inchauspe G, Lemon S, Spaan W. 1995. Almost the entire 5′ non-translated region of hepatitis C virus is required for cap independent translation. *FEBS Lett 365*:115–119.

Rijnbrand R, van der Straten T, van Rijn PA, Spaan W, Bredenbeek P. 1997. Internal entry of ribosomes is directed by the 5′ noncoding region of classical swine fever virus and is dependent on the presence of an RNA pseudoknot upstream of the initiation codon. *J Virol 71*:451–457.

Rozen F, Edery I, Meerovitch K, Dever TE, Merrick WC, Sonenberg N. 1990. Bidirectional RNA helicase activity of eucaryotic initiation factors 4A and 4F. *Mol Cell Biol 10*:1134–1144.

Sambrook J, Fritsch EF, Maniatis T. 1989. *Molecular cloning. A laboratory manual*, 2nd ed. Cold Spring Harbor, New York: Cold Spring Harbor Laboratory Press.

Stormo GD, Schneider TD, Gold LM. 1982. Characterization of translation initiation sites in *E. coli*. *Nucleic Acids Res 10*:2971–2996.

Tratschin JD, Moser C, Ruggli N, Hofmann MA. 1998. Classical swine fever virus leader proteinase N^{pro} is not required for viral replication in cell culture. *J Virol 72*:7681–7684.

Tsukiyama-Kohara K, Iizuka N, Kohara M, Nomoto A. 1992. Internal ribosome entry site within hepatitis C virus RNA. *J Virol 66*:1476–1483.

Wang C, Sarnow P, Siddiqui A. 1993. Translation of human hepatitis C virus RNA in cultured cells is mediated by an internal ribosome-binding mechanism. *J Virol 67*:3338–3344.

Zhao WD, Wimmer E, Lahser FC. 1999. Poliovirus/hepatitis C virus (internal ribosome entry site) chimeric viruses: Improved growth properties through modification of a proteolytic cleavage site and requirement for core sequences but not core-related polypeptides. *J Virol 73*:1546–1554.